JOURNAL OF PROPULSION AND POWER
Vol. 10, No. 4, July–Aug. 1994

Experimental Study of a Model Gas Turbine Combustor Swirl Cup, Part I: Two-Phase Characterization

Hongyu Wang,* Vincent G. McDonell,† William A. Sowa,‡ and Scott Samuelsen§
University of California, Irvine, Irvine, California 92717

The behavior of droplets and the continuous phase (i.e., gas in the presence of the droplets) downstream of a 3x model gas turbine combustor dome swirl cup is characterized via phase Doppler interferometry in the absence of reaction. The goal is to improve the understanding of droplet-gas interaction in a complex flow typical of that produced by engine hardware. Three components of continuous phase and droplet velocities were measured along with droplet size. The measurements reveal that 1) at the exit plane of the swirl cup, more uniform and finer droplets are produced relative to the atomizer alone, 2) both the continuous phase and droplets recirculate, 3) the region downstream of the swirl cup into which droplets join the recirculation is correlated with droplet size, and 4) significant slip velocities exist between the continuous phase and the droplets which are also correlated with droplet size and reflect a strong momentum exchange between the phases.

I. Introduction

SWIRL-INDUCED recirculating flows are commonly used in gas turbine combustors to enhance mixing and improve reaction stability. Much work has been conducted to understand single phase swirling flows with and without the presence of reaction.[1-6] Recently, experiments have been performed to characterize droplet[7-9] and continuous-phase[10] flowfields with a single swirling airstream introduced coannularly to spray nozzles. This past research has provided useful insight into continuous-phase and droplet behavior associated with atomizers in the presence of aerodynamic swirl, and shown the challenges in the study of droplet-gas interaction in complicated flows.

In order to further enhance mixing of the two phases, dual coaxial swirling streams are used. One of these applications is the General Electric (GE) Aircraft Engine CFM56 engine combustor swirl cup, in which the primary and secondary swirlers provide coaxial, counter-rotating airstreams.

The present study employs a 3x scale swirl cup patterned after production gas turbine hardware to provide improved resolution of spatial gradients while maintaining the basic structure of the swirl cup flowfield. The gas-phase characteristics of this swirl cup are discussed separately[6] and the droplet dynamics are presented in Ref. 11. The goal of the present study, combined with those in Refs. 6 and 11, is to provide the insight of the physics of droplet-gas interaction and a data base in support of numerical model verification.

To achieve this goal, three objectives were established: 1) characterize the continuous-phase and discrete-phase flowfields downstream of the swirl cup, 2) study the influence of the swirl cup on the droplet size distribution, and 3) provide an understanding of the effect of the gas-phase flowfield on the droplet motion.

Received March 20, 1992; revision received Oct. 21, 1993; accepted for publication Nov. 21, 1993.

*Research Assistant, UCI Combustion Laboratory. Student Member AIAA.

†Senior Research Engineer, UCI Combustion Laboratory. Member AIAA.

‡Associate Director, UCI Combustion Laboratory.

§Professor, Director, UCI Combustion Laboratory. Associate Fellow AIAA.

II. Experiment

A. Test Facilities

The model combustor swirl cup is shown in Fig. 1. This is a 3x scale model of the GE CFM56 combustor where R_p = 29.3 mm. A hollow-cone simplex atomizer with 90-deg spray angle was mounted in the center of the swirl cup. The swirl cup generates two coaxial, counterswirling airstreams. Looking from the top of the swirl cup, the primary air rotates clockwise and the secondary air rotates counterclockwise. The swirl cup mounting plate was attached to a PVC pipe (0.3 m long × 0.154 m i.d.) inside of which a 0.106-m-thick, 0.154 m-o.d. polycarbonate honeycomb sheet (with 0.006-m cell i.d.) was placed 0.050 m above the swirl cup to provide a uniform velocity profile at the entrance plane of the swirlers. The assembly was mounted onto a traverse which provides movement in three orthogonal directions. The swirl cup position was monitored with a three-axis digital indicator which is accurate to within 0.01 mm.

Water was used in lieu of liquid fuel. The atomizer operated at a mass flow rate of 0.010 kg/s with a pressure drop of 827 kPa across the nozzle. The mass flow rate of air was 0.154 kg/s, corresponding to a 3-kPa pressure drop, providing an air-to-liquid ratio of about 15. The swirl cup discharged into a quiescent, unconfined environment.

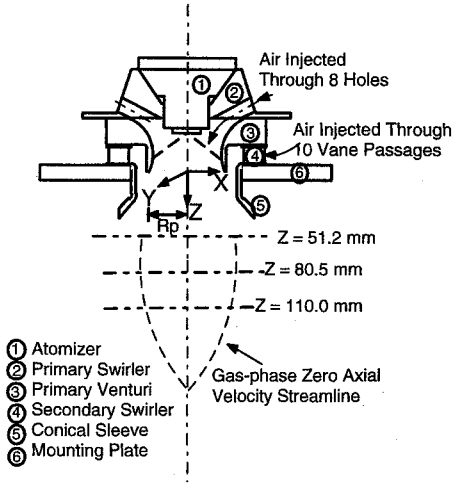

Fig. 1 3x model combustor swirl cup.

Table 1 Characteristics of phase Doppler interferometer

Transmitter
0.5145-μm line (U, D)[a]
Fringe spacing, 9.88 μm
Waist, 187.17 μm
0.4880-μm line (V or W)[a]
Fringe spacing, 9.84 μm
Waist, 177.53 μm
Receiver
1000-mm f/9.3 collection lens
238-mm focusing lens
100-μm spatial filter
30-deg forward collection angle

[a]U, V, W, and D are the axial, radial, tangential velocity components and droplet diameter, respectively.

B. Diagnostics

A two-component phase Doppler interferometer [Phase Doppler Particle Analyzer (PDPA), Aerometrics Model 3100-S] was used to measure 1) the continuous-phase velocities and 2) the size and velocities of the droplets. The optical setup is delineated in Table 1. A Spectra-Physics 2016 multiline argon ion laser was used at a laser power of 1.0 W (all lines). A TSI Model 3906 six-jet atomizer introduced a salt solution into the air plenum feeding the swirl cup to provide seed. In this study, the continuous-phase and droplet velocities were measured separately. The continuous-phase velocities measured in the presence of spray were determined by isolating the statistics to droplets below 4.1 mm in diam, which was the smallest size class detected with the PDPA setup in this study. Note that, for the present study, only the air issuing from the swirl cup was seeded. This is due to insufficient seeding available for large volume of surrounding air. As a result, measurements near the edge of the flow from the swirl cup are biased towards the higher velocities of this stream (i.e., concentration bias). However, the regions of interest (mixing between the two streams produced by the two swirlers) reflects minimal bias.

III. Results and Discussion

A. Size and Data Rate

The swirl cup is designed to provide uniform and fine droplets. A portion of the droplets issue from the nozzle and convect downstream directly. The remaining spray impinges onto the inner surface of the primary venturi, forming a liquid film which is then reatomized due to the strong shearing of the primary and secondary airstreams at the edge of the primary venturi. Figure 2 shows the length mean diameter D_{10} and the Sauter mean diameter D_{32}. In Fig. 2 as well as the remaining figures, the axes labels correspond to the orientation shown in Fig. 1 and the origin of the axes corresponds to the center of the primary venturi exit plane.

More fine droplets are detected in the region close to the centerline due to 1) preferential recirculation of small droplets and 2) the structure of the spray produced by the simplex atomizer. A sharp increase in D_{10} and D_{32} is observed at the periphery of the spray at the axial location, Z = 110 mm. This is attributed to the larger droplets from either atomizer or the breakup of liquid film at the edge of venturi that have sufficient radial momentum to penetrate through the swirling airstreams.

As shown in Fig. 3, at Z = 51.2 mm, the presence of the swirl cup and swirling air reduces 1) the variation in droplet size as a function of radial position, and 2) the width of the spray. The spray D_{32} near the centerline increases in the presence of the swirl cup because medium-size droplets are driven to the centerline by the recirculating flow produced in this

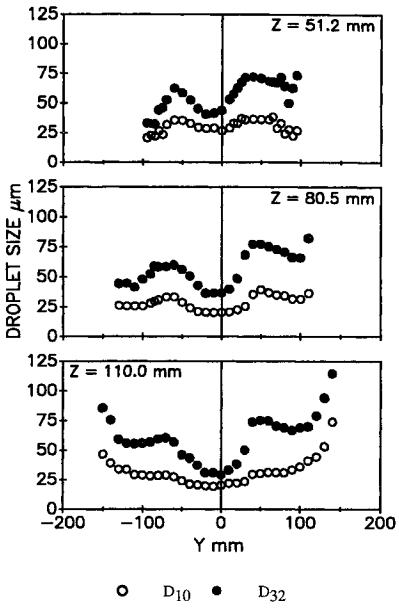

Fig. 2 Droplet size D_{10} and D_{32}.

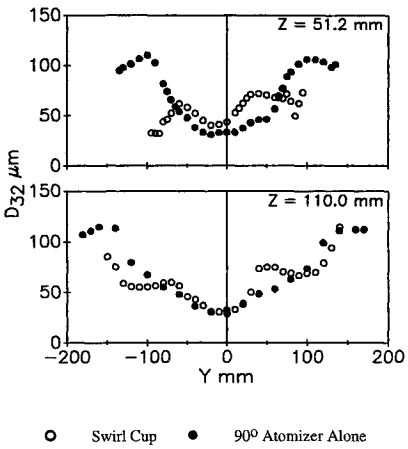

Fig. 3 Droplet size comparison.

case. At Z = 110 mm, each case exhibits similar sizes at a given location, but the swirl cup produces fine differences in structure as indicated by the local maximums at $Y = \pm 50$ mm. These local maxima are associated with the reatomization of liquid off the primary venturi.

Figure 4 presents radial profiles of the sampling rate of droplets of different sizes. The hollow nature of the spray in the presence of the swirling airstreams is evident at Z = 51.2 mm, however, it is quickly weakened further downstream due to dispersion of droplets by the swirling airstreams. The data rate of different droplet size classes peaks around the shear layer between the flow issuing from the swirl cup and the surrounding air, suggesting that this region features large droplet concentrations and high volume fluxes. The sharp increase in D_{10} and D_{32} at Z = 110.0 mm and $|Y| > 100$ mm is due to the penetration of larger droplets through the swirling air.

B. Mean Velocities

Radial profiles of droplet mean axial velocity at three axial locations are shown in Fig. 5. The width of the region in which the droplets recirculate is correlated with the droplet size. Small droplets are more likely to be convected back towards the inlet than are the larger droplets. The axial slip velocity (the difference of mean axial velocities between the droplets of different sizes and the continuous phase) is also correlated with the droplet size. The large axial slip velocity indicates a strong axial momentum exchange between the phases. Note

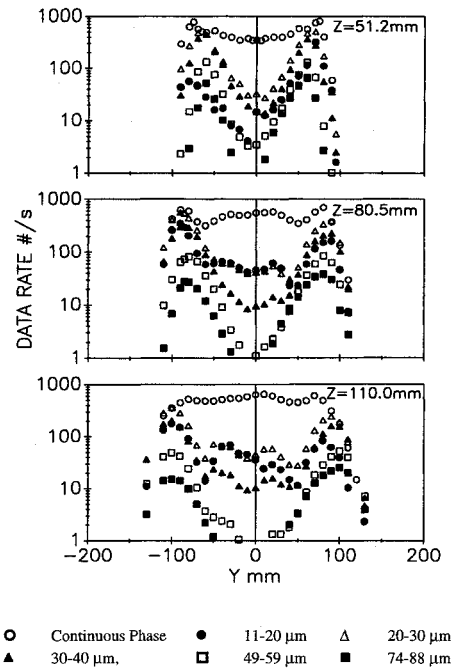

Fig. 4 Data rates.

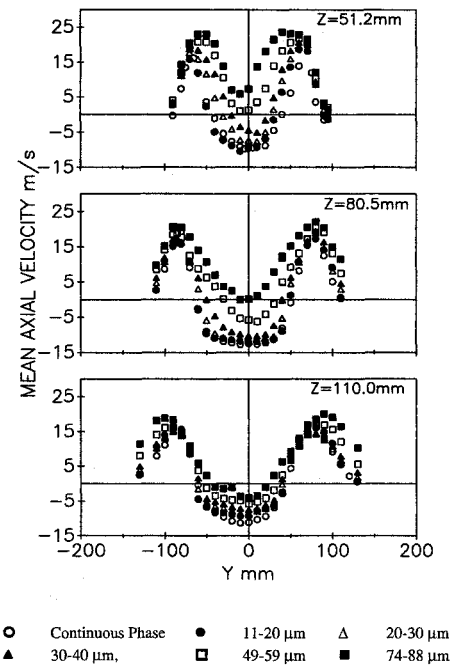

Fig. 5 Mean axial velocity.

that the slip velocity decreases as the mixing process develops downstream.

Figure 6 presents radial profiles of the mean radial velocities. In this figure, positive values on the $+Y$ side and negative values on the $-Y$ side indicate velocities away from the centerline. The radial slip velocity is not as great as the axial slip velocity at $Z = 51.2$ mm because the centrifugal force acting upon the droplets, whether they travel in the clockwise or counterclockwise direction, is radially outwards. Further downstream, the slip velocity increases in the shear layer because the decrease in radial velocity of the larger droplets is slower than the smaller droplets and the continuous phase. This is more evident at $Z = 110.0$ mm where large droplets continue to move away from the centerline while the continuous-phase and smaller droplets, not able to overcome the negative radial pressure gradient, follow the contraction of the recirculation zone towards the centerline.

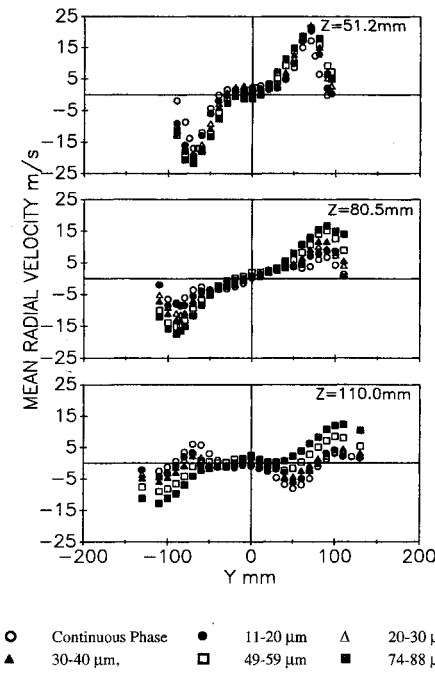

Fig. 6 Mean radial velocity.

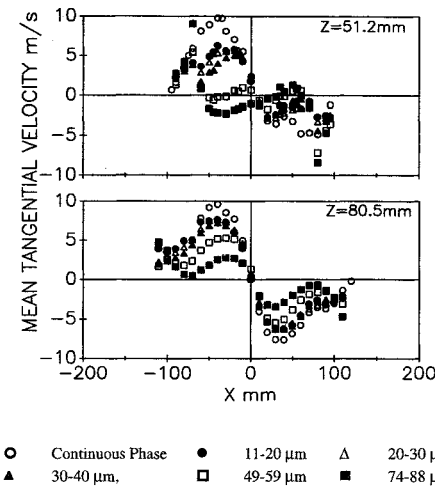

Fig. 7 Mean tangential velocity.

Figure 7 presents the mean tangential velocities. In this figure, positive values on the $-X$ side and the negative value on the $+X$ side represents counterclockwise rotation looking from the top of the swirl cup. At $Z = 51.2$ mm, the tangential velocity profile of the smaller droplets (e.g., with diameter between 10 – 40 mm) reveals one peak inside the recirculation zone and another peak outside (this is more clearly shown on the $-X$ side). This complex structure is a result of three sources of smaller droplets which contribute to the distributions measured at $Z = 51.2$ mm: 1) droplets recirculating while swirling counterclockwise; 2) droplets produced from the edge of the venturi which are dominated by the counterclockwise-swirling secondary air; and 3) droplets injected directly from the atomizer, which are initially dominated by the clockwise rotating primary air.

At the shear layer, a local minimum in the mean tangential velocity exists because of the relative contributions from the three sources. At $Z = 80.5$ mm, fewer small droplets are produced by the third source described above, and only mean velocities associated with counterclockwise rotation are observed. This indicates that, at $Z = 80.5$ mm, the flow is dominated by secondary airstream.

The larger droplets (diameters over 50 μm) display tangential velocities that are correlated with the point of origin

of the droplets. Few larger droplets are recirculated, thus only two of the above sources contribute to measurements of these droplets made at $Z = 51.2$ mm. The droplets swirling clockwise likely come directly from the atomizer and retain the momentum imparted by the primary airstream. The larger droplets that are swirling counterclockwise likely come from the edge of the primary venturi where the momentum is imparted by the secondary airstream.

The larger droplets display their maximum axial velocity where the tangential velocity is nearly zero, while the smaller droplets display a maximum tangential velocity where the axial velocity is almost zero. This demonstrates that the larger droplets with greatest axial momentum are less affected by the swirling airstreams in the tangential direction, whereas some of the smaller droplets in the vicinity of the zero streamline move almost only in the r-Θ plane.

C. Fluctuating Velocities

Figure 8 shows the rms of the axial velocity (termed in this study "fluctuating velocity"). The peak values of the axial velocity fluctuations are similar for different droplet size classes. Inside the recirculation zone ($|Y| < 55$ mm), the largest droplets display the greatest fluctuation in axial velocity. This is attributed to the superposition of 1) variation of measured droplet velocity due to the arrival of droplets from different origins (e.g., venturi or atomizer) and the different droplet history (e.g., from upstream or downstream); and 2) fluctuations due to the turbulence of the gas phase.

The fluctuating radial velocities are shown in Fig. 9. The continuous-phase velocity fluctuations are greater than those of the droplets in the region where measurements were conducted. This is due to the unique direction of the centrifugal force acting upon the droplets, regardless of their origin. The peaks of the radial velocity fluctuations are further away from the centerline compared with the corresponding axial and tangential velocity fluctuations, with an exception at $Z = 110.0$ mm. Here, the increasing radial velocity fluctuation in the region close to the centerline is due to the influence of the stagnation point of the recirculation zone, where large-scale unsteadiness (e.g., precession) intensifies the radial velocity fluctuation.

Figure 10 shows the tangential velocity fluctuations of the continuous phase and the droplets of different sizes. The peaks of the tangential velocity fluctuation are located at the shear

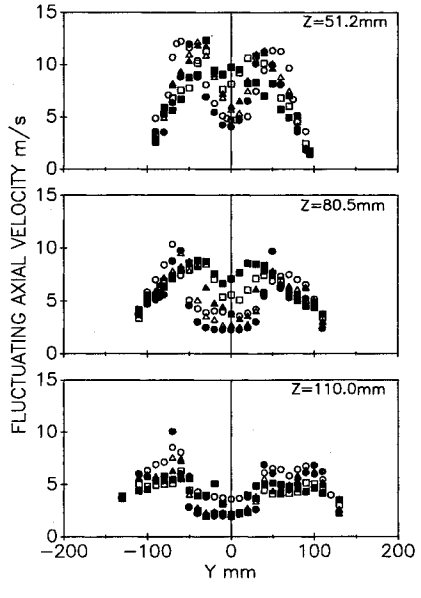

Fig. 8 Fluctuating axial velocity.

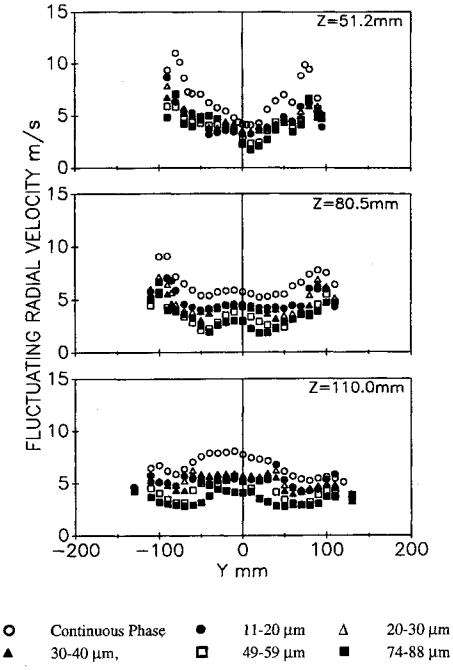

Fig. 9 Fluctuating radial velocity.

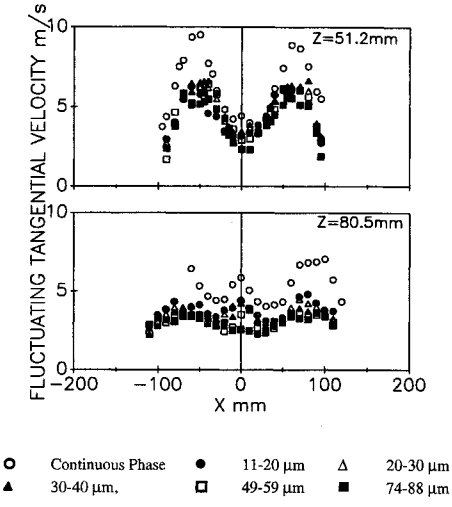

Fig. 10 Fluctuating tangential velocity.

layer where the primary and secondary airstreams counteract. Due to the strong shearing resulting from the counterswirling, the mixing in the tangential direction is fast and at $Z = 80.5$ mm, the distribution of the tangential velocity fluctuations for different size-class droplets is quite uniform. At the centerline, a local maximum is observed for the gas phase, which is also associated with precession.

Examination of the fluctuating axial, radial, and tangential velocities reveals that the turbulence properties of this flowfield are not isotropic.

The mean and fluctuating axial and radial velocities along the centerline are presented in Fig. 11. Smaller droplets join the recirculation zone from a greater portion of the centerline region. Also, the larger droplets join the recirculating flow over a smaller region located relatively far downstream. The fluctuating axial velocity decreases downstream due to a reduction in the recirculating strength.

A local maximum in the fluctuating radial velocity is observed at the end of the recirculation zone which is attributed to the dynamics of this structure. The mean radial velocities of both the continuous phase and droplets are less than 3 m/s at the centerline. The nonzero values are attributed to 1) large gradients in tangential velocity (recall Fig. 7), and 2) a

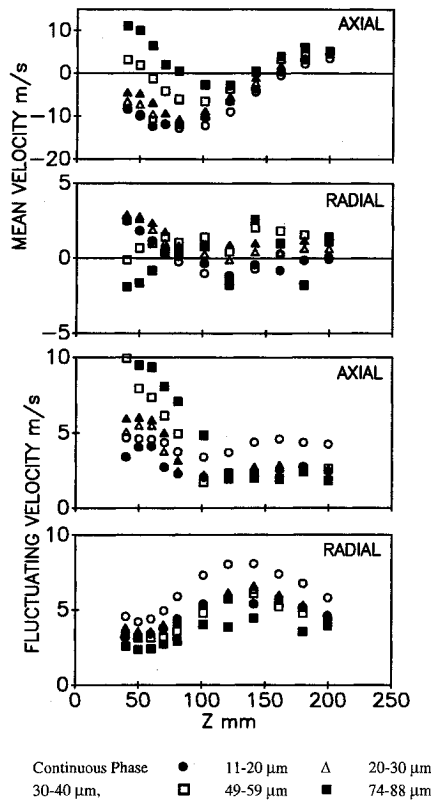

Fig. 11 Distributions along the centerline.

modest mismatch of the aerodynamic and geometric centerlines.

IV. Conclusions

1) At the exit plane of the swirl cup, smaller more uniformly distributed droplets are produced relative to the atomizer alone. Farther downstream, both cases have similar sizes although the details of the profiles reveal important differences.

2) Both the continuous phase and droplets recirculate. The volume from which the droplets recirculate is correlated with the droplet size.

3) Significant slip velocities are observed. The magnitude of the slip velocity depends on droplet size. Generally speaking, the larger the droplets, the greater their slip velocity. The prominent slip velocities indicate strong momentum exchange between the phases.

4) The droplet axial fluctuating velocity is greater than that of the continuous phase within the recirculation zone. This is due to the different origins and history of droplets, and the influence of local turbulence.

5) The continuous-phase turbulence property is anisotropic.

Acknowledgments

The authors acknowledge the financial support from General Electric Aircraft Engines and discussions with David Burrus as program liason, and the assistance from C. T. Brown and H. D. Crum during the test.

References

[1]Oven, M. J., Gouldin, F. C., and McLean, W. J., "Temperature and Species Concentration Measurements in a Swirl-Stabilized Combustor," *Seventeenth Symposium (Int'l) on Combustion*, The Combustion Inst., Leeds, England, UK, Oct. 1976, pp. 363–374.

[2]Vu, B. T., and Gouldin, F. C., "Flow Measurements in a Model Swirl Flow," *AIAA Journal*, Vol. 20, No. 5, 1982, pp. 652–659.

[3]Habib, M. A., and Whitelaw, J. H., "Velocity Characteristics of Confined Coaxial Jets with and Without Swirl," *Journal of Fluid Engineering*, Vol. 102, 1980, pp. 47–53.

[4]Gouldin, F. C., Depsky, J. S., and Lee, S. L., "Velocity Field Characteristics of a Swirling Flow Combustor," AIAA Paper 83-0314, May 1983.

[5]Samimy, M., and Langenfeld, C. A., "Experimental Study of Isothermal Swirling Flow in a Dump Combustor," *AIAA Journal*, Vol. 26, No. 12, 1988, pp. 1442–1449.

[6]Mehta, J. M., Shin, H. W., and Wisler, D. C., "Mean Velocity and Turbulent Flow Field Characteristics Inside an Advanced Combustor Swirl Cup," AIAA Paper 89-0215, Jan. 1989.

[7]Cameron, C. D., Brouwer, J., and Samuelsen, G. S., "A Comparison of Spray Characterization in an Isothermal Chamber and in a Model Gas Turbine Can Combustor," *Proceedings of the 4th International Conference on Liquid Atomization and Spray Systems*, Sendai, Japan, 1988, pp. 145–152.

[8]McDonell, V. G., Wood, G. P., and Samuelsen, G. S., "A Comparison of Spatially Resolved Drop Size and Drop Velocity Measurements in an Isothermal Chamber and a Swirl Stabilized Combustor," *Twenty-First Symposium (Int'l) on Combustion*, The Combustion Inst., Pittsburgh, PA, 1986, pp. 685–695.

[9]Bachalo, W. D., Rudoff, R. C., and Sankar, S. V., "Time-Resolved Measurements of Spray Drop Size and Velocity," *Liquid Particle Size Measurement Techniques*, 1st ed., Vol. 2, American Society for Testing and Materials, Philadelphia, PA, 1990, pp. 209–224.

[10]Breña de la Rosa, A. B., Bachalo, W. P., and Rudoff, R. C., "Spray Characterization and Turbulence Properties in an Isothermal Spray with Swirl," *Journal of Engineering for Gas Turbines and Power*, Vol. 112, Jan. 1990, pp. 60–66.

[11]Wang, H. Y., Sowa, W. A., McDonell, V. G., and Samuelsen, G. S., "Experimental Study of a Model Gas Turbine Combustor Swirl Cup, Part II: Droplet Dynamics," *Journal of Propulsion and Power* Vol. 10, No. 4, 1994, pp. 446–452.